Video Article

# Measurement of Tension Release During Laser Induced Axon Lesion to Evaluate Axonal Adhesion to the Substrate at Piconewton and Millisecond Resolution

Massimo Vassalli[1], Michele Basso[2], Francesco Difato[3]

[1]Institute of Biophysics, National Research Council of Italy

[2]Dipartimento di Sistemi e Informatica, Università di Firenze

[3]Department of Neuroscience and Brain Technologies, Istituto Italiano di Tecnologia

Correspondence to: Francesco Difato at Francesco.Difato@iit.it

URL: http://www.jove.com/video/50477
DOI: doi:10.3791/50477

Keywords: Bioengineering, Issue 75, Biophysics, Neuroscience, Cellular Biology, Biomedical Engineering, Engineering (General), Life Sciences (General), Physics (General), Axon, tension release, Laser dissector, optical tweezers, force spectroscopy, neurons, neurites, cytoskeleton, adhesion, cell culture, microscopy

Date Published: 5/27/2013

Citation: Vassalli, M., Basso, M., Difato, F. Measurement of Tension Release During Laser Induced Axon Lesion to Evaluate Axonal Adhesion to the Substrate at Piconewton and Millisecond Resolution. *J. Vis. Exp.* (75), e50477, doi:10.3791/50477 (2013).

## Abstract

The formation of functional connections in a developing neuronal network is influenced by extrinsic cues. The neurite growth of developing neurons is subject to chemical and mechanical signals, and the mechanisms by which it senses and responds to mechanical signals are poorly understood. Elucidating the role of forces in cell maturation will enable the design of scaffolds that can promote cell adhesion and cytoskeletal coupling to the substrate, and therefore improve the capacity of different neuronal types to regenerate after injury.

Here, we describe a method to apply simultaneous force spectroscopy measurements during laser induced cell lesion. We measure tension release in the partially lesioned axon by simultaneous interferometric tracking of an optically trapped probe adhered to the membrane of the axon. Our experimental protocol detects the tension release with piconewton sensitivity, and the dynamic of the tension release at millisecond time resolution. Therefore, it offers a high-resolution method to study how the mechanical coupling between cells and substrates can be modulated by pharmacological treatment and/or by distinct mechanical properties of the substrate.

## Video Link

The video component of this article can be found at http://www.jove.com/video/50477/

## Introduction

Optical microscopy is one of the less invasive imaging system available to observe living cells. With the exploitation of effects such as radiation pressure (as in optical tweezers[1]), or high-energy photon flux (as in laser dissector[2]), this technology was extended to nano-manipulation. The optical imaging system furnishes a precise control to visualize and manipulate sub cellular targets[3]. At the same time, thanks to the accurate calibration of the delivered laser power, optical tools accomplish either soft or invasive sample manipulation with unprecedented reproducibility.

Several laboratories integrated, in the same experimental setup, optical tweezers and laser dissector in order to ablate organelles[4], to fuse together different cells[5], or to stimulate cells by optically driven cargos[6,7]. While optical tweezers, after calibration of the optical stiffness, allow for the control of applied force to the cell on a piconewton scale, laser dissection systems can modulate optical manipulation, which ranges from membrane photo-poration to ablation of single organelles or dissection of sub-cellular structures. However, laser dissection calibration relies on qualitative assessment of the entity of optical manipulation with respect to the energy delivered to the sample, mainly based on image analysis illustrating morphological changes caused to the specimen[8]. In the presented method, we demonstrate how to perform force spectroscopy measurement during the laser axonal dissection of a developing neuron, to quantify, on piconewton scale, the force produced by an altered equilibrium in the cytoskeleton structure of a sub-cellular compartment[9]. Cultured neurons adhere to the substrate, and polarize during development. The polarization phase occurs during the first five days *in vitro*. At stage two of polarization, one of the extruding neurites becomes longer, and it will differentiate to become the axon[10]. Axonal elongation in response to towing force at the growth cone has been previously modeled by Dennerl's model[11]. Recently, this model has been extended[12] to include the role of neurite adhesion to the extracellular matrix substrates. This biophysical model, proposed after experimental observations[13], showed that pulling forces on growth cone, propagating along the neurite, are modulated by focal adhesions to the substrate. Likewise, axonal lesion produces a local release of tension propagating toward the cell body. Thus, we proposed that measuring such released tension in a location along the axon between the lesion and the cell soma offers the possibility to assess the dampening outcome of unaffected focal adhesions.

We calibrate the necessary energy photon-flux of the laser dissector to control the extent of the inflicted axonal damage, from complete transection to partial lesion. Following the calibration, we repeated partial lesion to the axons of several differentiating neurons and developed the protocol to quantify the tension release, and thus obtained a quantitative parameter to estimate the adhesion of the axon to the substrate[14].

In the present work, we describe in detail the developed protocol, which represents a precise experimental procedure to evaluate and compare with piconewton sensitivity the axonal adhesion to the substrate in different experimental conditions such as chemical treatment[14], or different types of cell culture support.

## Protocol

# 1. Optical Setup

The entire optical system was described earlier[15]. Briefly, the optical tweezers system is based on an ytterbium continuous wave (CW) fiber laser operating at 1064 nm (IPG Laser GmbH). A spatial light modulator (SLM) (LCOS-SLM, model X10468-07 - Hamamatsu) varies the phase of the incoming IR laser beam to control the position of the trapping focus spot on the culture dish by computer generated holograms. The freely available Blue-tweezers software (web link on equipment table) generated holograms projected on the spatial light modulator. The interferometer for force spectroscopy measurements was based on a four-quadrant photodiode (QPD, S5980 with C5460SPL 6041 board - Hamamatsu) and a photodiode (PD, PDA100A-EC - Thorlabs).

The laser dissection source was a pulsed sub-nanosecond UV Nd:YAG laser at 355 nm (PNV-001525-040, PowerChip nano-Pulse UV laser - Teem Photonics). An acousto-optic modulator (MQ110-A3-UV, 355 nm fused silica -AA-Opto-electronic) controlled the power of the UV laser delivered to the sample.

The holographic optical tweezers and laser micro-dissector were integrated on a modified upright microscope (BX51 - Olympus) equipped with a 60X, 0.9 NA water dipping objective.The stage of the microscope is composed of a 3-axis linear DC motor micro-positioning system (M-126.CG1, Physics-Instruments) carrying a separate 3-axis piezoelectric nano-positioning stage (P-733.3DD, Physics-Instruments) to combine coarse movement of the sample with the sub-nanometer resolution of the piezo-stage. The microscope stage system was equipped with two control loops synergistically acting to maintain the trapping focus spot at the right position, depending on the selected working mode (position or force clamp, static or dynamic)[16]. In particular, an internal feedback loop acts on a piezoelectric stage, to keep the bead at a selected distance from the trap center. The other external loop controls the position of the motorized stage to exploit the region spanned by the piezo-actuator on a larger area than its available stroke[17]. When the piezo-stage reaches the limit of the available stroke in one direction, the external loop moves the micro stage in the opposite direction, thus the piezo recovers toward its central position because it is tracking the trapped bead adhered to the sample. When the piezo-stage reaches the central position of its course range, the micro stage halted. Further details of the system are reported in Guiggiani *et al*[16,17].

A Peltier device (QE1 resistive heating with TC-344B dual channel heater controller - Warner Instruments) controls the temperature of the cell culture under the microscope (37 °C). In the culture, pH and humidity were maintained at physiological conditions by aerating a custom-designed polydimethylsiloxane (PDMS) sleeve (integrating the microscope objective) with humidified carbogen (95% $O_2$, 5% $CO_2$).

# 2. Cell Culture Preparation

All the experimental protocols were approved by the Italian Ministry of Health. Primary cultures were obtained from hippocampi of mice (C57BL6J, Charles River) at embryonic day 18 (E18).

1. Neurons were plated at a concentration of 25,000 cells/ml on glass-bottom Petri dishes (P35G-0-14-C - MaTek Corporation). The low concentration of cultured cells is needed to avoid the formation of a dense network already in the first days *in vitro*. At the mentioned cell concentration, the likelihood of finding isolated cells with a longer neurite not connected to other cells is much higher.

# 3. Bead Coating

1. Polymer microspheres (Ø 4 µm, COOH-terminated- Bangs Laboratories, product code PC05N/6700) were coated with poly-D-lysine following the procedure described in the polyLink Protein Coupling Kit (Polysciences, product code 19539). The beads are coated with the same molecule used to cover the culture support and favor cells adhesion.

# 4. Choose Isolated Neuron. Detach A Bead from the Culture Substrate, Trap and Move it Next to the Neuron

1. Put the culture Petri dish on the microscope stage. After setting the focus on the sample by stage motion, correct the position of the illuminating objective condenser to set Kohler-illumination. Aligning the illumination optics to set the Kolher-illumination condition is necessary to improve the bright field imaging quality. Using such alignment conditions, it is also necessary to maximize the IR laser collection efficiency (through objective condenser), from the scattering trapped probe, to perform its interferometric tracking by the QPD and PD.
2. Pipette a few µl of the coated microsphere stock solution into the culture dish. Microspheres will deposit and adhere to the culture substrate. The number of µl injected into the culture dish depends on the microsphere concentration of the stock solution. The ideal condition is to have between one and two microspheres per imaging field of view. When too many microspheres are added to the culture dish, they can already attach randomly to the cultured neurons.
3. Move around in the culture dish, searching for an isolated neuron with a longer neurite (the axon), and save the position of the microscope stage.

4. Move around and search for a bead adhered to the culture support.
5. Turn on the IR trapping laser. At this stage, no holograms are projected on SLM, and the position of IR laser spot coincides with the UV laser spot position. Set the axial position of the IR spot 2-3 µm above the culture support surface, by microscope stage motion.
6. Set the UV laser power delivered to the sample to less than 1 µW. The UV laser dissector has been previously calibrated[14]:

   5-6 µW the glass support is ablated

   4 µW a neuronal connection is completely dissected

   2.5 µW a neurite is partially lesioned

   ‹ 1 µW a shock wave is produced in the culture dish. The optical shock wave is strong enough to detach the bead from the glass support.
7. Turn on the UV laser, while leaving the IR laser on, and move the UV spot above the adhered bead by microscope stage motion. The bead detaches from the surface, and it is trapped by the IR laser. Then, turn off the UV laser.
8. Move the trapped bead several micrometers above the glass support (20-30 µm). Lifting the bead to this position will prevent it from contacting other cells while it is being moved toward the previously chosen neuron. Bring the bead to the previously saved stage position. Set the stage speed to a low value (10 µm/sec) so the drag fluid force does not exceed the optical trapping force.

## 5. Move the Trap Position with Respect to the Laser Dissector Spot and Axon Position by Computer Generated Hologram, and Calibrate the Optical Tweezers Stiffness

1. Move the bead toward the glass support to visualize the axon. The bead is held above the cell to avoid contact with it (about 5 µm above the glass support).
2. Move the microscope stage to move the UV focus spot on the center of the width of the axon. Save the current stage position.
3. Move the IR focus spot position by computer-generated hologram. In this step, the stage is halted in the position chosen in the previous step. When the computer generated hologram is projected on the SLM, the trapped bead is moved with respect to the axon. We move the IR laser spot to have the trapped bead aligned on the center of the neurite, with the UV laser spot centered on the same neurite too. The IR spot and thus the trapped bead are positioned along the neurite 5-10 µm away from the UV spot. We move the position of the IR with respect to the UV spot depending on the neurite geometry. In case the optical tweezers are not equipped with an SLM system, the position can be varied by tilting mirrors, or acoustic optic deflectors, on the IR optical path. The IR laser spot may be positioned 5-10 µm away from the UV spot to avoid optical interaction of the dissecting beam with the trapped probe, which could influence its Brownian motion and alter the force spectroscopy traces.
4. After defining the new IR spot position with respect to UV spot and axon position, move the stage to position the trapped bead away from the axon and avoid collision with it. Move the axial position of the trapped bead to about 2 µm above the cover glass.
5. Align the QPD to center the interference fringes on it: x and y QPD differential signals are zeros when the QPD is centered. Acquire 5 sec of the Brownian motion of the trapped bead by the interferometer, at 50 KHz sampling rate. Obtain the stiffness (pN/nm) and sensitivity (V/nm) of the optical trap by the power spectrum method[18].

## 6. Attach the Bead to the Axon. Perform Axotomy and Simultaneous Force Measurement

1. Raise the trapped bead position about 4 µm above the cover glass, and move it to the previously saved stage position (see step 3.2).
2. Move the trapped bead down toward the axon until it contacts the neurite. The collision between the trapped bead and the axon is monitored by the z QPD signal detecting displacement of the trapped bead in the axial direction.
3. Wait 10 sec with the trapped bead pushed against the axon to favor its adhesion to the neurite membrane.
4. Move the micro stage to displace the trapped bead from the axon, and thus verify its adhesion to the cell membrane. If the bead adhered, it escapes from the optical trap.
5. Move back the laser trap on the adhered bead and switch on the force-clamp loop with force condition equal to zero. In such a way, the piezo-stage repositions the bead, attached to the cell, on the optical trap center. If the system does not have a feedback loop control, the laser trap position can be moved by the microscope stage to center it on the adhered probe. The center of the trap is reached when the QPD signals are the same as when the bead is trapped and not adhered to the cell (x and y QPD signals equal to zero, and the z QPD signal gives the same voltage sum of the four quadrants as when the bead is trapped far from any surface) .
6. Set a force-clamp condition on the z axis, positioning the trapping laser slightly over the center of the bead (about 100 nm), to generate a pretension on the adhered trapped probe. In case the system is not equipped with a force-clamp control, the optical trap position can be raised up at steps of 25 nm by the microscope stage. The z QPD signal allows monitoring. Therefore, use this signal to set the position of the laser trap with respect to the adhered probe. Such pre-tension is needed to sense the strain on the membrane after the axonal lesion, and the consequent decrease of Brownian motion of the adhered probe. A similar approach has been proposed to measuring the release of tension in a membrane tether by video imaging[19].
7. Switch-off the force-clamp feedback to measure the force on the adhered probe in the position-clamp condition (the piezo-stage is blocked).
8. Start simultaneous recording of the trapped probe positions through the interferometer (20 KHz sampling frequency), and the cell during laser axotomy time-lapse bright-field imaging (20 Hz frame rate).
9. Turn on the UV laser to deliver laser pulses until a lesion becomes visible on the image of the axon (Usually 200-400 optical pulses are needed. Energy per pulse: 25 nJ), then turn off the UV laser.
10. Continue recording by the interferometer for about 3 min, until the x, y and z QPD traces reach a plateau.

## 7. Quantify the Total Tension Release

1. Convert the recorded QPD traces (in Volts) by the calibrated sensitivity of the optical trap, to obtain the respective traces in nanometers.

2. Filter the x, y, and z displacement traces by a high pass filter with cut off at 10 Hz.
3. Calculate the total variance of the filtered traces representing the Brownian motion of the trapped bead. Calculate the variance at 25 msec steps for overlapping time windows of 500 msec (10,000 data points)[20]. The high pass filtering of traces excludes the changes of Brownian motion due to the membrane fluctuation or cortical actin motion. The Brownian motion of the bead is reduced by the optical forces and the adhesion forces on the cell membrane. When the membrane is strained because of the release of tension its viscosity is increased, and thus the Brownian motion of the bead, detected immediately after axotomy, starts to decrease.
4. Define t0: the beginning of decrease of the Brownian motion variance, after the delivery of UV laser energy. The time instant t0 indicates the beginning of membrane strain.
5. Define t1: the end of decrease of the Brownian motion variance (when it reaches a plateau). The time instant t1 indicates the end of membrane strain.
6. Perform video tracking of debris or a scratch on the cover glass support, to measure any drift of the sample during the force measurement. To track the particle on the glass support, we first apply thresholds to the bright-field images, to obtain a stack of binary images with the particle in white on a black background. Then, we track the particle center of mass with sub-pixel accuracy (using the freeware ImageJ software).
7. Subtract the measured drift from the displacement QPD traces. Multiply the drift-corrected QPD traces by the respective calibrated optical stiffness ($k_x$, $k_y$, $k_z$) to obtain the Fx, Fy, Fz traces in piconewtons.
8. Calculate the total force trace as $F_{tot} = \sqrt{(Fx^2+Fy^2+Fz^2)}$.
9. Calculate the total release of force between t0 and t1 as $F_{released} = F_{tot}(t1) - F_{tot}(t0)$. The force measured at t0 has to be subtracted because it is due to the displacement of the probe from the trap center, when the bead adheres to the neurite.
10. Calculate the neurite contact area between the trapped bead and the UV laser spot position: on the bright field image measure the long (L) and short (D) axes of the neurite between the trapped bead and the UV laser spot position. The axon contact area is $A_{axon} = L \times D$.
11. Normalize the total released force $F_{released}$ by the axon contact area $A_{axon}$.

## Representative Results

The cell generates traction forces on the substrate by its focal adhesions. Force generated by cytoskeletal elements are in equilibrium with the counteracting force of the culture substrate. After laser induced lesion of the neurite, some of the tensed cytoskeleton cables are disrupted and their equilibrated tension is released because the opposing force of the substrate adhesion is eliminated. The released tension is partially distributed on the unaffected focal adhesions, and the bead attached to the cell membrane, held in an optical trap, measures the portion of such release not counteracted by cytoskeletal elements anchoring the cell to the substrate (see schematic **Figure 1**).

We report, in **Figure 2**, a representative result of the above-described experimental protocol. The neuron, in **Figure 2a** left panel, presents a longer neurite, which identifies the axon of the differentiating neuron. In **Figure 2a** right panel, the same neuron is shown after the induced axonal lesion (indicated by the white arrow). **Figure 2b** shows the recorded bead displacement traces in x, y, and z directions. **Figure 2c** reports the video tracking of a scratch on the glass support, to take into account and eliminate the stage drift during the measurement.

In **Figure 3a**, on the left panel, we show the lesioned neurite, and the white line upstream the lesion site, where we calculate the kymograph of the neurite diameter during the tension release measurement. On the right panel is the kymograph, showing how the neurite diameter slightly increases immediately after the lesion, and then becomes thinner due to the release of tension toward the cell soma. In **Figure 3b**, we quantify the kymograph result. The neurite appears brighter with respect to the background since we positioned the attached bead in the focus center of the objective, and therefore the axon is slightly out of focus. Indeed, by reporting the sum of pixel intensities along the kymograph line at each frame of the time-lapse video recording, we obtain an estimate of the neurite diameter during the release of tension. On panel **3c**, we report the total variance of the attached bead during the tension release, calculated based on the traces recorded by the interferometer (in **Figure 2b**) after high pass filtering at 10 Hz cut-off frequency. We can observe that the variance increases with the neurite diameter during accumulation of material upstream of the lesion site. Then, the variance starts to decrease (at t0 in **Figure 3c**) when the membrane is strained, and the neurite diameter decreases too. The variance decrease reaches a plateau (at t1 in **Figure 3c**), when the tension release ceases. After t1, the Brownian motion starts to increase because of membrane relaxation possibly due to exocytosis[21] (see **Figure 3c**).

In **Figure 4a**, the white box indicates the estimation of the neurite contact area $A_{axon}$ with the culture support. $A_{axon}$ is calculated between the UV laser spot position and the center of the trapped probe. **Figure 4b** reports the amplitude trace of the total released force $F_{released}$ obtained after multiplying the drift-corrected QPD displacement traces (in **Figure 2b**) by the respective calibrated optical trap stiffness ($k_x$, $k_y$, $k_z$). We calculate the difference between force measured at time t1 and t0 (ΔpN in **Figure 4b**), and then we divide by $A_{axon}$, to obtain the tension released in terms of $pN/\mu m^2$.

By repeating the same protocol on different neurons in the sample, we can start sessions of experiments on several cultures treated with chemical factors or plated on different supports, and finally compare the average value obtained in the distinct experimental conditions. In **Figure 5**, we show the release of tension after axonal lesion is dampened by focal adhesions on the substrate, thus a higher tension release value means an axon less adhered to the substrate. Because we induce a partial, and not complete, lesion of the axon, we investigated the dependence of the measured tension release on the total energy delivered, and on the neurite contact area between the lesion site and the trapped bead. We sought to destroy more cytoskeletal elements by delivering a higher number of light pulses, and consequently induce a higher release of tension. Otherwise, with an increased neurite contact area, we expected to measure a lower amount of tension release. In **Figure 5**, we show that the dependency on the two above-mentioned parameters is not clear. Therefore, we deduced that the induced partial lesion (with the previously calibrated low energy per pulse; see protocol step 4.5), is related to the dimension of the ablation spot[8], which does not vary when using the same microscope objective and the same energy per pulse at the sample. Moreover, the fact that the release of tension is not correlated to the contact area is not surprising because it is well known that such parameters do not represent a good estimate of the cell adhesion to the substrate, as focal adhesions occupy only 1% of the basal surface[22].

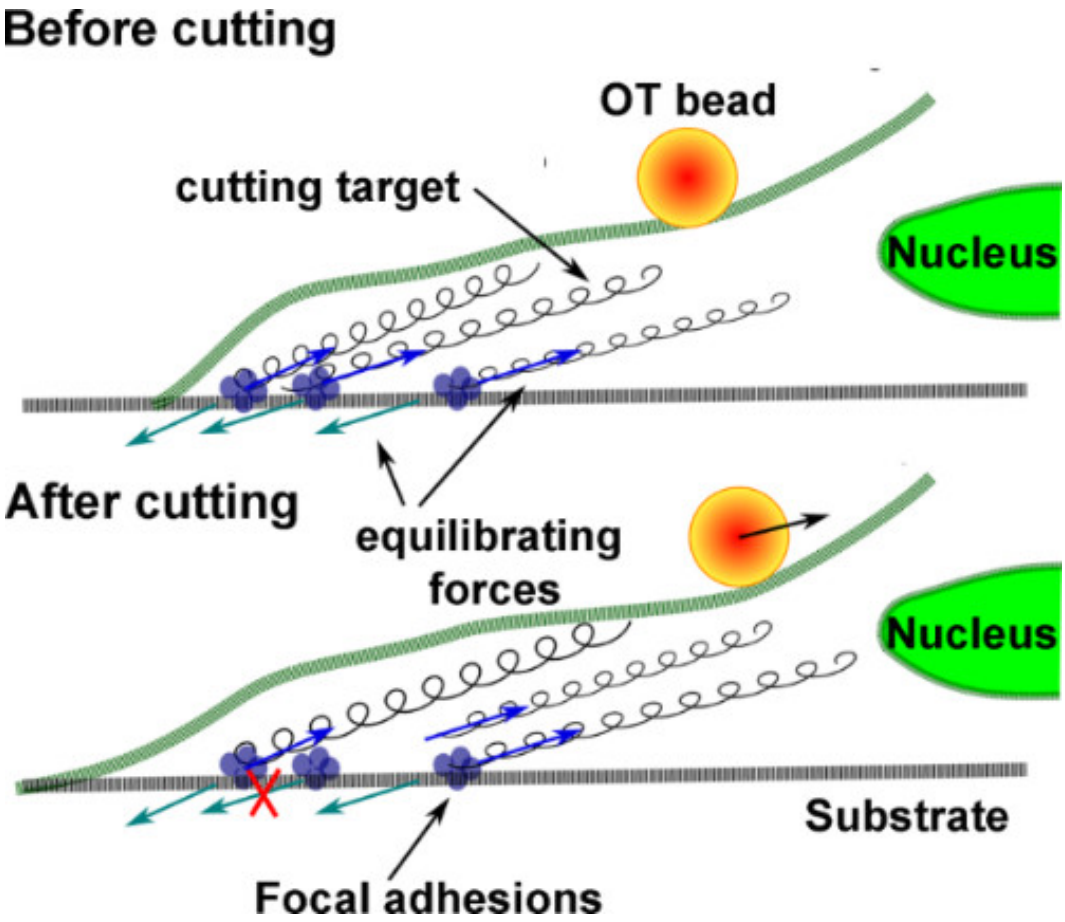


**Figure 1. Graphical representation of the disrupted cytoskeleton equilibrium during laser axotomy.** A cell adheres to a substrate by focal adhesions. Blue arrows specify traction forces generated by cytoskeletal elements (indicated by springs). Light-blue arrows indicate the counteracting forces generated by the rigid culture substrate. In a simplified scenario, before lesion, the cytoskeletal and substrate forces are paired and equilibrated. After laser-induced lesion of the neurite, the connections between some springs and the substrate are disrupted. Thus, the substrate is no longer counteracting the traction force of the cytoskletal element. The trapped bead, attached to membrane, tracks the direction of the released cytoskeleton forces.

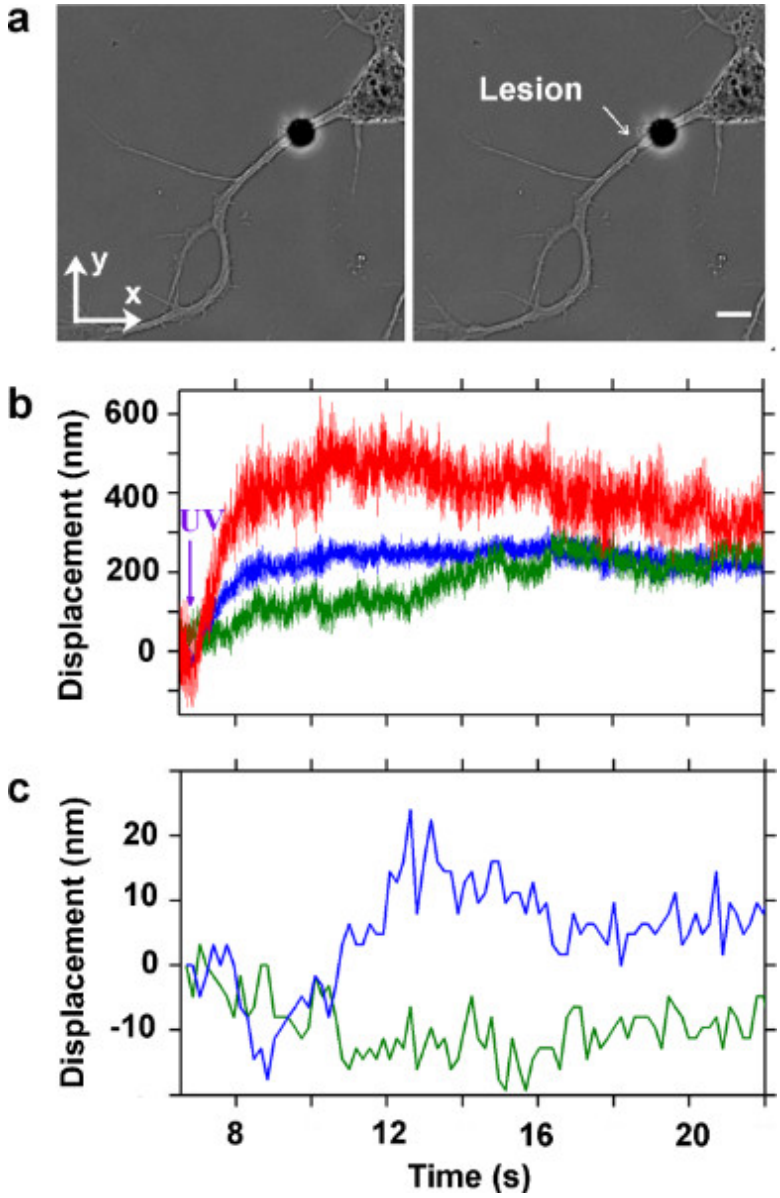


**Figure 2. Interferometric tracking of a trapped bead, attached to the membrane of the axon of a hippocampal neuron during laser induced lesion. (a)** Bright field images acquired during ablation of an axon. Before the lesion on the left panel. After the lesion on the right panel. A poly-D-Lysine coated bead is attached to the membrane (polystirene bead, Ø 4 µm) and held in an optical trap. Average power of the IR laser at the sample is 14 mW. White arrow indicates the lesion site. Bar is 5 µm. **(b)** Recorded traces by back focal plane interferometry of the bead position in the optical trap. Blue, green and red traces represent the bead position along x, y, and z axes, respectively. Sampling rate is 20 kHz. **(c)** Displacement of a scratch on the culture support measured by video tracking to monitor the stage drift. Blue and green traces are the x and y positions obtained by video tracking. Frame rate is 5.5 Hz.

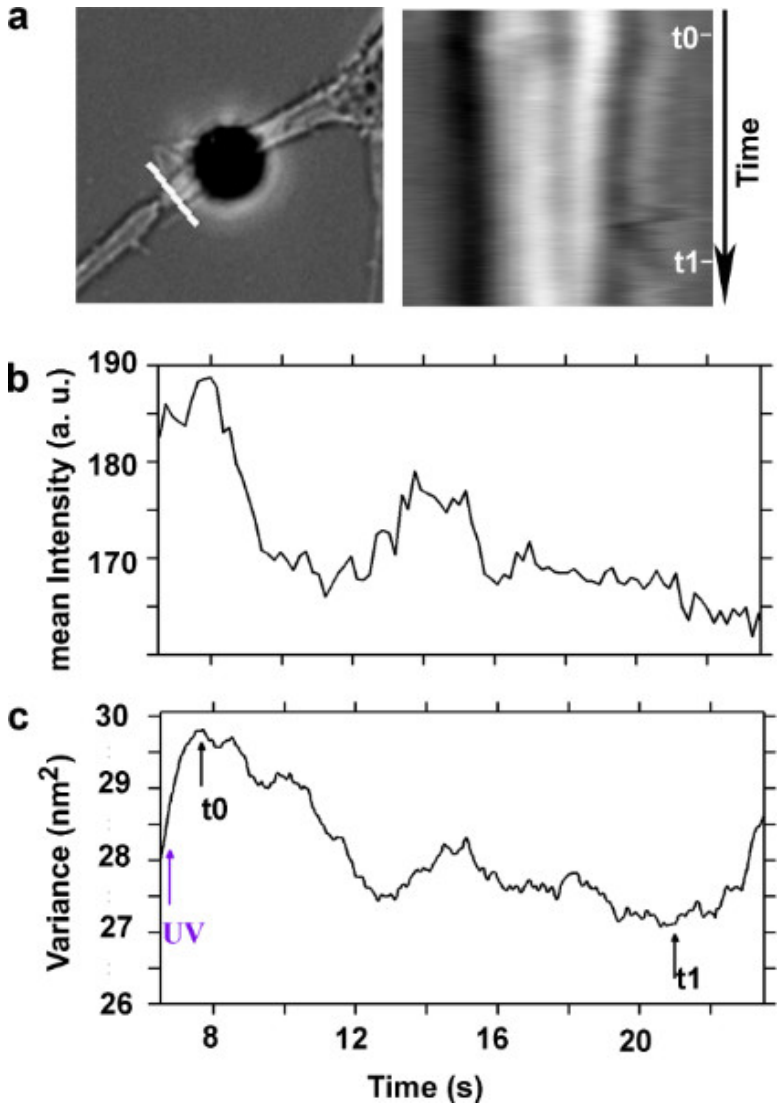


**Figure 3. Analysis of the axon diameter during the tension release, and the membrane strain of the lesioned axon. (a)** Bright field image of the lesioned axon, on the left panel. The white line perpendicular to the axon indicates the position where a kymograph is computed. On the right panel, kymograph of the axon diameter, upstream of the lesion site. Each row of the kymograph corresponds to 0.18 sec. **(b)** Sum of pixel intensities of each row of the kymograph representing an estimate of the axon diameter during the tension release. **(c)** Total variance of the Brownian motion of the bead attached to the axon (t0 and t1 indicate respectively the beginning and the end of tension release in the axon after dissection).

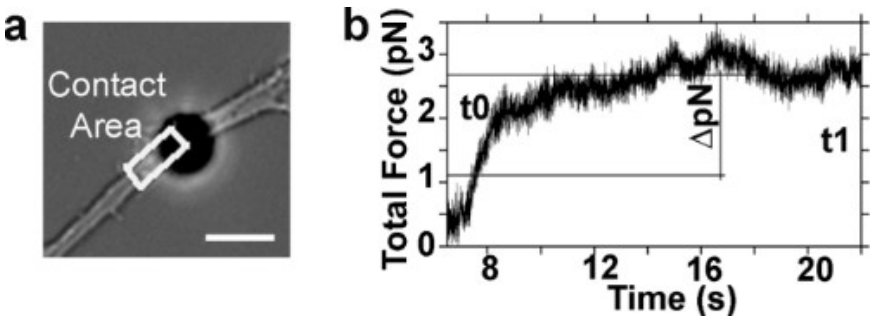


**Figure 4. Quantification of the tension released after axotomy. (a)** Bright field image of the lesioned axon. The white box indicates the estimate of the neurite contact area between the lesion site and the center of the trapped bead. **(b)** Trace of the total amplitude of the force measured after axotomy ($F_{tot}$= √($Fx^2$+$Fy^2$+$Fz^2$)). Fx, Fy, and Fz were calculated by Hooke's law (F = kx), where the displacement traces are the ones shown in **Figure 2b**. The stiffnesses, in the three orthogonal directions, of the optical trap were calculated by the power spectrum method ($k_{x,y}$ = 7.9 pN/μm, $k_z$ = 2.3 pN/μm). ΔpN indicates the measured released force between the time instants t0 and t1.

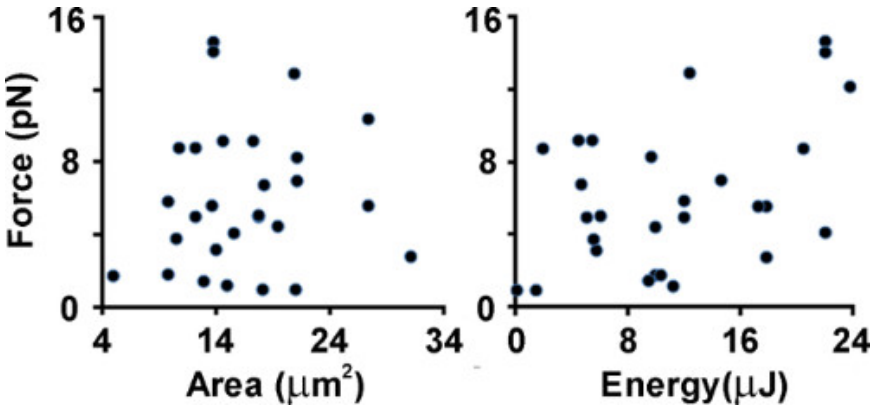


**Figure 5. Dependence of measured tension release on the amount of energy delivered to the sample, and on the neurite contact area.** Data from 26 experiments performed on the axons of mouse hippocamapal neurons at 3 DIV. **(a)** Scatter plot of tension release versus neurite contact area between lesion and trapped bead locations. **(b)** Scatter plot of tension release versus total amount of energy delivered to the sample neurite contact area.

## Discussion

We report in this work a quantitative method to compare the neurite adhesion to the culture substrate, by performing simultaneous force spectroscopy measurement during laser induced cell lesion. The measured release of tension is related to the degree of adhesion of the cell to the substrate: cells with a higher number of focal adhesions should release less tension. Measuring the release of tension in terms of piconewtons provides a physical quantity by which to evaluate the axonal adhesion to the culture support in different experimental conditions[14].

Several laboratories integrated a laser dissector with an optical tweezers system, adopting distinct optical designs[23]. Our choice was a setup with fixed optical path and microscope stage motion. To accomplish this, we introduce a spatial light modulator in the IR laser beam path to move the trapping spot with respect to the UV laser position. Although galvanometric mirrors allow steering the laser focus position without moving the sample, they can introduce mechanical noise in the system affecting the force spectroscopy measurements. Moreover, we decided to re-position the IR laser focus in the sample, since Brownian motion analysis permits a fast re-calibration of the optical stiffness. Moving the UV laser spot position onto the sample can produce spherical aberrations affecting the quality of the UV focus spot itself, which are negligible only for small displacements of the beam from its central position. Therefore, modification of the optical properties of the laser dissector could require a *de novo* calibration of the delivered laser power versus damage to the entity.

By force spectroscopy measurement, we could observe that the tension release is composed of a fast phase of a few seconds, and a slow phase that could last some tens of seconds. As reported in previous work[14], sometimes the slow phase could last a few minutes. For that reason, we had to correct the force measurement by video tracking a scratch on the culture support. In the future, a better approach would be to cancel stage drift with a feedback loop, which auto-corrects the microscope stage position by video or interferometric tracking of a bead attached to the cover glass. This type of configuration, already reported in the literature, requires a second laser beam centered on the attached bead, and ensures stage stabilization with sub-nanometer precision[24,25].

In the future, we want to apply the developed protocol to compare the axonal adhesion to the culture support at different stages of differentiation and in different pathological conditions to provide a quantitative assay for pharmacological treatment. Moreover, the same protocol could apply to the design of implantable scaffolds, to compare the neuronal adhesion to different types of materials with distinct mechanical or chemical properties[26].

## Disclosures

The authors declare that they have no competing financial interests.

## Acknowledgements

Alberto Guiggiani for developing the real time control system, Evelina Chieregatti and Hanako Tsushima for insightful discussions, Giacomo Pruzzo and Alessandro Parodi for the development of custom electronics and software, and Claudia Chiabrera and Marina Nanni for their expert advice and assistance in cell culture preparation.

## References

1. Ashkin, A. & Dziedzic, J.M. Optical Trapping and Manipulation of Viruses and Bacteria. *Science.* **235**, 1517-1520 (1987).
2. Berns, M.W., Aist, J., *et al.* Laser microsurgery in cell and developmental biology. *Science.* **213**, 505-513 (1981).
3. Nguyen, Q.T., Olson, E.S., *et al.* Surgery with molecular fluorescence imaging using activatable cell-penetrating peptides decreases residual cancer and improves survival. *Proc. Natl. Acad. Sci. U.S.A.* **107**, 4317-4322 (2010).
4. Stiess, M., Maghelli, N., *et al.* Axon extension occurs independently of centrosomal microtubule nucleation. *Science.* **327**, 704-707 (2010).
5. Steubing, R.W., Cheng, S., Wright, W.H., Numajiri, Y., & Berns, M.W. Laser induced cell fusion in combination with optical tweezers: the laser cell fusion trap. *Cytometry.* **12**, 505-510 (1991).
6. Pinato, G., Raffaelli, T., D'Este, E., Tavano, F., & Cojoc, D. Optical delivery of liposome encapsulated chemical stimuli to neuronal cells. *J. Biomed. Opt.* **16**, 095001-095004 (2011).
7. Kress, H., Park, J.G., *et al.* Cell stimulation with optically manipulated microsources. *Nat. Methods.* **6**, 905-909 (2009).
8. Berns, M.W. A history of laser scissors (microbeams). *Methods Cell Biol.* **82**, 1-58 (2007).
9. Difato, F., Dal, M.M., *et al.* Combined optical tweezers and laser dissector for controlled ablation of functional connections in neural networks. *Journal of Biomedical Optics.* **16**, 051306_1-8 (2011).
10. Goslin, K. & Banker, G. Experimental observations on the development of polarity by hippocampal neurons in culture. *J. Cell Biol.* **108**, 1507-1516 (1989).
11. Dennerll, T.J., Lamoureux, P., Buxbaum, R.E., & Heidemann, S.R. The cytomechanics of axonal elongation and retraction. *J. Cell Biol.* **109**, 3073-3083 (1989).
12. O'Toole, M. & Miller, K.E. The role of stretching in slow axonal transport. *Biophys. J.* **100**, 351-360 (2011).
13. O'Toole, M., Lamoureux, P., & Miller, K.E. A physical model of axonal elongation: force, viscosity, and adhesions govern the mode of outgrowth. *Biophys. J.* **94**, 2610-2620 (2008).
14. Difato, F., Tsushima H., *et al.* The formation of actin waves during regeneration after axonal lesion is enhanced by BDNF. *Nature Scientific Reports.* **1** (183), (2011).
15. Difato, F., Schibalsky L., Benfenati, F., & Blau, A. Integration of optical manipulation and electrophysiological tools to modulate and record activity in neural networks. *International Journal of Optomechatronics.*, 191-216 (2011).
16. Guiggiani, A., Torre, B., *et al.* Long-range and long-term interferometric tracking by static and dynamic force-clamp optical tweezers. *Opt. Express.* **19**, 22364-22376 (2011).
17. Guiggiani, A., Basso M., Vassalli M., & Difato, F. RealTime Suite: a step-by-step introduction to the world of real-time signal acquisition and conditioning. 3rd Real Time Linux Workshop, (2011).
18. Neuman, K.C. & Block, S.M. Optical trapping. *Review of Scientific Instruments.* **75**, 2787-2809 (2004).
19. Togo, T., Krasieva, T.B., & Steinhardt, R.A. A decrease in membrane tension precedes successful cell-membrane repair. *Mol. Biol. Cell.* **11**, 4339-4346 (2000).
20. Kress, H., Stelzer, E.H., *et al.* Filopodia act as phagocytic tentacles and pull with discrete steps and a load-dependent velocity. *Proc. Natl. Acad. Sci. U.S.A.* **104**, 11633-11638 (2007).
21. Togo, T. Disruption of the plasma membrane stimulates rearrangement of microtubules and lipid traffic toward the wound site. *J. Cell Sci.* **119**, 2780-2786 (2006).
22. Huang, H., Kamm, R.D., & Lee, R.T. Cell mechanics and mechanotransduction: pathways, probes, and physiology. *Am. J. Physiol. Cell Physiol.* **287**, C1-11 (2004).
23. Scrimgeour, J., Eriksson, E., & Goksor, M. Laser surgery and optical trapping in a laser scanning microscope. *Methods Cell Biol.* **82**, 629-646 (2007).
24. Carter, A.R., King, G.M., *et al.* Stabilization of an optical microscope to 0.1 nm in three dimensions. *Appl. Opt.* **46**, 421-427 (2007).
25. Capitanio M., Cicchi R., & Pavone F. Position control and optical manipulation for nanotechnology applications. *The European Physical Journal B.* **46**, 1-8 (2005).
26. Roach, P., Parker, T., Gadegaard, N., & Alexander, M.R. Surface strategies for control of neuronal cell adhesion: A review. *Surface Science Reports.* **65**, 145-173 (2010).

 